Current Research in Food Science 8 (2024) 100739

Contents lists available at ScienceDirect

Current Research in Food Science

journal homepage: www.sciencedirect.com/journal/current-research-in-food-science

Composite alginate-based hydrogel delivery of antioxidant pumpkin protein hydrolysate in simulated gastrointestinal condition

Zeinab Nooshi Manjili [a], Alireza Sadeghi Mahoonak [a,*], Mohammad Ghorbani [a], Hoda Shahiri Tabarestani [a], Vahid Erfani Moghadam [b]

[a] Department of Food Science and Technology, Gorgan University of Agricultural Sciences and Natural Resources, Gorgan, Iran
[b] Department of Medical Nanotechnology, Faculty of Modern Technologies, Golestan University of Medical Sciences, Gorgan, Iran

ARTICLE INFO

Handling Editor: Dr. Quancai Sun

Keywords:
Pumpkin seed protein hydrolysate (PSPH)
Alginate-based hydrogel
Release rate
FTIR
SEM
Encapsulation efficiency

ABSTRACT

Pumpkin seeds are rich in protein (24–36.5%). Some of them are consumed as nuts, while others are regarded as waste and used for feeding animals. Protein hydrolysates from pumpkin seeds possess some bioactive properties, such as anti-oxidant activity. In this work, various composite alginate hydrogels contain Aloe vera, CMC, and tragacanth have been employed to protect PSPH against degradation in simulated gastrointestinal digestion (SGI) and regulate its release rate. The encapsulation efficiency of PSPH in plain alginate and beads with Aloe vera, CMC, and tragacanth combinations was 71.63, 75.63, 85.07, and 80.4%, respectively. The release rate of the plain alginate beads was %30.23 in the SGF and %52.26 in the SIF, and decreased in the composite-based beads. The highest decreasing rate in the antioxidant activity during SGI was observed in free PSPH, and the decreasing rate slowed down in the alginate-based composites. The swelling rate in plain alginate was %-23.43 and %25.43 in the SGF and SIF, respectively, and increased in the composite-based beads. The FTIR spectra of hydrogels before and after loading with PSPH showed identical absorption patterns and were similar to each other. Based on the data for SEM, it was revealed that substituting other polymers in polymer combinations with alginates resulted in a porosity reduction of the beads and smoother and more uniform surfaces. Based on the results, the combination of polysacchared with alginate could protect and increase the applicability of PSPH as a functional component in the food industry.

1. Introduction

Pumpkin is a perennial plant that belongs to the family *Cucurbitaceae* and different varieties are available worldwide. One of the most popular types of pumpkin is *C. maxima*. High protein content (24–36.5%) in pumpkin seed (Rezig et al., 2016) and the existence of many bioactive substances, such as oils, sterols, polyamines and antioxidants in pumpkin seeds, have motivated researchers to explore the use of them in traditional medicine systems for a long time (Aktaş et al., 2018; Aziz et al., 2018; Cho et al., 2014). Recent studies suggest that hydrolysates from pumpkin seed protein possess antioxidant properties (Mazloomi--Kiyapey et al., 2019; Sitohy et al., 2020) and also enhance zinc bioavailability (Lu et al., 2021). Unfortunately, these by-products are either discarded as household or agricultural-industrial waste or used to feed animals. Therefore, based on their nutritional and biological properties, these seeds hold great potential for being used as food ingredients (Amin et al., 2019; Bučko et al., 2015; Rezig et al., 2016).

Hydrogels are three-dimensional polymer networks with crosslinks that can take in a large amount of water or biological fluids. According to Hacker and Mikos (2011), hydrogels can be formed by either chemical or physical methods. Hydrogels may be formed in the presence of divalent cations, including calcium, strontium and barium. However, as a result of being a naturally occurring ion in the human body, calcium ions are most common since they do not cause any allergic reactions. Additionally, compared to the other ions mentioned, it has no adverse toxic effect, according to Zhang and Zhao (2020). There are two kinds of hydrogels: natural and synthetic. Natural hydrogels are based on natural polymers such as chitosan, alginate, cellulose, proteins and gum Arabic. In comparison with their synthetic counterparts, natural hydrogels are more biodegradable. This property has made them widely used in the food industry, medicine and biotechnology for making sensors, targeted drug release carriers, absorption systems for dyes and metal ions, contact lenses, etc. (Ahmed, 2015; Kabiri et al., 2011). In the area of drug and bioactive compound delivery, hydrogels are capable of being loaded

* Corresponding author.
E-mail address: sadeghiaz@gau.ac.ir (A.S. Mahoonak).

https://doi.org/10.1016/j.crfs.2024.100739
Received 13 February 2024; Received in revised form 3 April 2024; Accepted 16 April 2024
Available online 23 April 2024

with highly dosed bioactive compounds as well as controlling their sustained release. As a result, stable hydrogels with appropriate structures exhibit high stability and releases a small amount of the content in acidic stomach conditions while releasing most of it in intestinal conditions (Swamy and Yun, 2015).

Alginate is a naturally occurring anionic hydrophilic polymer obtained from brown seaweed and has been employed in several food uses due to its various functions, for example, forming film, gelling effect, thickening and stabilization (Shah, 2020). Alginate can be applied in diverse forms such as films, hydrogels, microspheres, fibers and microcapsules across different industries, including cosmetics/beauty products, health/wellness products like drug delivery systems or implants, and scaffolds for tissue regeneration and biomaterials applications (Prasathkumar and Sadhasivam, 2021). Numerous studies have examined the utilization of alginate-based delivery systems as matrices for antioxidant peptides. For example, Betancur-Ancona et al. (2021) used *Guazuma ulmifolia* gum and sodium alginate to micro-coat antioxidant peptides from *Phaseolus lunatus*. On the other hand, Cano-Sampedro et al. (2021) encapsulated sprouted soybean protein hydrolysate using alginate and xanthan gum under colonic fermentation conditions with controlled release. In a separate study done by Gómez-Mascaraque et al. (2016), the effect of micro-hydrogels on whey protein hydrolysate during micro-encapsulation was assessed for their stability in the digestive system as well as their potential use in yoghurt products. The usage of alginate has downsides too, like bioactivity, mucosal adhesion and low shelf life (Perez et al., 2014). In addition, the gel formed has low mechanical strength, the loading capacity for bioactive compounds is also low, and it releases loaded molecules quickly at intestinal pH (Bušić et al., 2018).

Aloe Vera mucilage is a hydrocolloid made up mainly of water (99%), which can be used as a thickening agent with good emulsifying properties that may be appropriate for encapsulation (Medina-Torres et al., 2019). Aloe Vera has some medicinal uses such as antimicrobial (Lorenzetti et al., 1964; Robson et al., 1982), anti-inflammatory (Hirata and Suga, 1977), analgesic (Fujita et al., 1976), cell-regenerative (Seyger et al., 1998), antioxidant (Yagi et al., 2003) and anticancer (Desai et al., 1996; Su et al., 2005). Thus, Sun's team designed this kind of nonwoven fabrics to act as a controlled release system (Sun et al., 2017).

An anionic polysaccharide, tragacanth gum, has a negative charge in a wide range of pH (Carpentier et al., 2022). Being a heterogeneous and highly branched complex polysaccharide, is the best description of tragacanth gum. Such non-food industries as pharmaceuticals and food products like sauce and ice cream often use this substance (Kurt et al., 2016). Tragacanth gum is also applied in the development of different drug delivery systems, such as micro or nano hydrogels (Hemmati et al., 2016; Hosseini et al., 2016).

Among the most widely used cellulose derivatives is carboxymethyl cellulose (CMC). This kind of cellulose derivative, when CH_2COOH groups are added to cellulose's molecular chain, leads to the production of carboxymethyl cellulose (CMC), which is an anionic linear polysaccharide. CMC edible coatings have been produced for food preservation because they can form a film excellently, are soluble in water, are safe, and are relatively less expensive (Yu et al., 2022). According to Ali's team findings, CMC is tasteless, biodegradable, not toxic, and soluble in both hot and cold water since its structure allows it to be broken down easily into simpler molecules (Ali et al., 2022).

Liang et al. (2016), by microencapsulation of epigallocatechin gallate inside niosomal vesicles and investigating its iron ion reduction property during digestion in simulated intestinal conditions, reported that the amount of antioxidant activity of the free and micro-encapsulated compounds within 2 h of digestion in the intestine decreased, but this decrease was less in the microencapsulated sample. Also, Hu et al. (2017) reported that by microencapsulating orange peel flavonoid compounds in pectin nanoparticles, their antioxidant power decreased during digestion in simulated intestinal conditions, and this decrease was greater in free flavonoid compared to microencapsulated flavonoid.

Bogdanova et al. (2022) increased the stability of calcium alginate hydrogel by adding some gelatin to it, which increased cell viability, increased ionic bonding and controlled release. Alvarado et al. (2019) investigated the encapsulation of antihypertensive peptides from whey proteins and their release under digestive conditions by three composite materials: alginate-collagen, gum Arabic alginate and alginate-gelatin. Their results showed that the highest encapsulation efficiency as well as the highest ACE inhibition rate after the digestive period were related to gum Arabic-alginate.

The main goal of this article is to investigate the protective effect of alginate-based composite hydrogels on the protection of PSPH and its release rate in the simulated digestive environment. This article can help researchers to choose the best formulation for their research.

2. Materials and methods

2.1. Materials

Tragacanth and Aloe Vera leaves were purchased from the local market (Gorgan, Iran). Sodium alginate, CMC, Calcium chloride ($CaCL_2$), Pancreatin (from porcine pancreas, 0.35 U/mg), Pepsin (from porcine gastric mucosa, 0.7 U/mg), Alcalase (2.97 U/ml), Brilliant Blue, Hexane, NaOH, Hydrochloric acid (HCL), Na_2HPO_4–NaH_2PO_4, Sodium chloride (NaCL), Potassium bromide (KBr), Methanol, DPPH, $FeCl_2$, Ferrozine, Sulfuric acid, Sodium phosphate, and Ammonium molybdate. All chemicals used were of analytical grade, were used as received without any further purification, and were obtained from Sigma-Aldrich and Merck.

2.2. Preparation of core materials (pumpkin seed protein hydrolysate)

Pumpkin fruit (*Cucurbita maxima* L.) was purchased from the local market (Astane-ashrafieh, Gilan, Iran). After separating the seeds manually, they were dried in an oven (Memmert, Germany) at 50 °C for 72 h.

2.2.1. Production of pumpkin protein concentrate

The pumpkin seeds, in a dry state, with husks, were ground by a mill (500 A, China) and passed through a 40-mesh sieve. Hexane was added to the powder at a ratio of 10:1 (V/W) and shaken (Noorsanat Ferdous, Iran) at 440 rpm for 4 h. The oil removal process continued until the residual oil was down to approximately 5%. Subsequently, any solvent that was left in the flour was separated using a vacuum oven (Memmert, Germany) at 40 °C for 24 h. After milling, the yielded flour was suspended in distilled water at a ratio of 1–10 (W/V), adjusted to pH 11 using 1 N NaOH solution in order to open the protein structure, and then stirred for 1 h by means of a magnetic stirrer (Jenway, UK). Then, the centrifugation (Combi-514R, South Korea) was carried out at 5000 rpm for 20 min at 4 °C. After collecting the supernatants, the pH was set to 4 using 1N hydrochloric acid. A repeated centrifugation cycle of 20 min at 5000 rpm and at temperature of 4 °C was performed again. At last, the pellet was freeze-dried (FDB 5503, South Korea) and maintained in a dry and cool environment. (Mazloomi-Kiyapey et al., 2019).

2.2.2. Microwave pretreatment

A solution containing 5% W/V of the pumpkin seed protein concentrate was prepared by adding the concentrate to 0.1 M phosphate buffer (100 gr/L) (Na_2HPO_4–NaH_2PO_4, pH 7.4) as a dispersion medium. It was left for 30 min to stir the dispersion and then subjected to microwave treatment (Daewoo, South Korea) with a power of 450–900 W for 30–90 s. It should be noted that after measuring the total antioxidant activity, microwave pretreatment at 600 W for 30 s was selected and applied as the optimum condition for pretreatment. Protein solutions pretreated with microwaves were used as substrates in enzymatic

hydrolysis experiments (Gohi et al., 2019).

2.2.3. Enzymatic hydrolysis

The response surface methodology was used to optimize the conditions of enzymatic hydrolysis. Alcalase and pancreatin enzymes were added in ratios from 0.5 to 2.5% of the protein substrate, and hydrolysis time was determined as an independent factor for each sample placed on a shaker incubator (VS-8480, South Korea) at a speed of 200 rpm within 20–190 min. The temperature and pH of hydrolysis were based on the optimal temperature and pH of each enzyme (pancreatin: 40 °C and pH = 7.4; alcalase: 50 °C and pH = 8). Then, protein solution was placed in a hot water bath (WNB 22, Germany) at a temperature of 85 °C for 15 min so that enzymes could be deactivated in them. Afterward, centrifugation took place (Combi-514R, South Korea) at 4000 rpm at 4 °C for 15 min before the supernatant was dried using a freeze dryer and stored at −20 °C until use (Nourmohammadi et al., 2017).

2.2.4. DPPH free radical scavenging activity

The hydrolysates were dissolved in distilled water at the optimal concentration (40 mg/ml). Then, 200 μl of the sample were mixed with 600 μl of methanol and 200 μl of DPPH (0.15 mM in methanol). After shaking vigorously for 2 min, it was kept at room temperature in a dark place for 30 min. The absorption was measured at 517 nm using a UV–vis (T80, UK) spectrophotometer. The control sample contained 800 μl of methanol and 200 μl of DPPH (0.15 mM). DPPH free radical scavenging activity is calculated according to Eq. (1) (Kanbargi et al., 2017).

$$\text{DPPH}\ (\%) = (\text{Blank absorbance} - \text{Sample absorbance})/\text{Blank absorbance} \times 100 \quad (1)$$

2.2.5. Iron ion chelation activity

200 μl of the sample was mixed with 10 μl of $FeCl_2$ (2 mM) and 600 μl of distilled water. Then 20 μl of ferrozine solution (5 mM) was added to the mixture and mixed vigorously for 2 min. After keeping the mixture at room temperature for 10 min, the color reduction due to iron chelating activity was recorded by measuring the absorbance at 562 nm. The control sample contained 800 μl of distilled water, 10 μl of $FeCl_2$, and 20 μl of ferrozine solution (5 mM). The percentage of chelating activity was calculated using Eq. (2) (Kanbargi et al., 2017).

$$\text{Iron Ion chelating activity}\ (\%) = (\text{Blank absorbance} - \text{Sample absorbance})/\text{Blank absorbance} \times 100 \quad (2)$$

2.2.6. Total antioxidant activity

100 μl of the sample with 1 ml of reagent (0.6 M sulfuric acid, 28 mM sodium phosphate, and 4 mM ammonium molybdate) was added into an Eppendorf tube and placed in a 90 °C water bath for 90 min. After cooling the samples, their absorbance was recorded at 695 nm. The control sample was double-distilled water. The higher absorption rate indicated the higher total antioxidant activity (Prieto et al., 1999).

2.3. Preparation of wall materials

Tragacanth gum was completely powdered (500 A, China), and sieved through a 40-mesh sieve. 30 g of the powder were mixed with 1000 ml of distilled water using a magnetic stirrer (Jenway, England) until dissolved fully. Its impurities were separated by centrifugation at a speed of 12,000 rpm for 20 min (Combi-514R, South Korea). The supernatant was put in an oven (Memmert, Germany) with a temperature set to 40 °C until complete dryness (Simas-Tosin et al., 2009).

For the preparation of aloe Vera mucilage, the leaves were completely washed and peeled off to reveal their thick gel, while inside the mixer, its gel was completely homogenized. After that it was placed into a tray which was then transferred into an oven (Memmert, Germany) and dried at 40 °C until it was fully dried.

2.4. Preparation of alginate-based delivery system

Ion gelation method was used for making hydrogel beads. First, a dispersion with a concentration of 2% sodium alginate and different combinations of polysaccharides such as aloe Vera, Tragacanth gum and CMC at a ratio of 80:20 were prepared for complete hydration by mixing them for 24 h at room temperature. This is followed by the addition of PSPH (40 mg/ml) to different wall materials dispersions in ratio1:1. Beads were formed by adding the resulting solution to 20 ml of $CaCl_2$ solution (5%) dropwise using a syringe (2 ml). After that, the beads were removed from the solution and washed with distilled water. Some of these beads were lyophilized (FDB 5503, South Korea), while the rest were used directly (Li et al., 2021).

2.5. Encapsulation efficiency

One ml of 0.1 M potassium phosphate buffer (pH = 8) was mixed with 100 mg of beads, after which it was stirred for 15 min using vortex (Maqsoudlou et al., 2020). Then using centrifugation (Combi-514R, South Korea) the beads separated from the dispersion at a speed of 15, 000 rpm for 20 min. The supernatant was suitably diluted and assayed by the Bradford method at a wavelength of 595 nm. Encapsulation efficiency was measured by Eq. (3) (Bradford, 1976; Guhagarkar et al., 2009).

$$\text{Encapsulation efficiency}\ (\%) = C_T - C_S/C_T \times 100 \quad (3)$$

where C_T was the total protein content and C_S was the supernatant protein content.

2.6. Release rate in simulated gastrointestinal digestion

Simulated gastric fluid (SGF) was prepared first with sodium chloride 0.2 g and pepsin 0.32% having a final pH of 2, while simulated intestinal fluid (SIF) was prepared by dissolving pancreatin 0.1% and potassium dihydrogen phosphate 50 mM to get a final pH of 7.4 (Basiri et al., 2017; Huang et al., 2023). The release rate was determined according to the Azad et al. (2020) method. Specifically, 10 ml of the simulated gastric medium were added to 1 g of beads, after which it was placed in a shaker incubator at a temperature of about 37 °C at a speed of 50 rpm for 2 h (VS-8480, South Korea). Sampling was done every 30 min. At the end, Bradford's method was employed to establish the magnitude of the release. Thereafter, 10 ml of simulated intestinal solution was added to each sample shaking continued at a speed of 50 rpm at a temperature of 37 °C and was further incubated for 4 h, followed by sampling every 60 min until the end point and measurement done using Bradford's technique.

2.7. Swelling

20 ml of simulated gastrointestinal environment were poured into a 1 gr sample of beads, which were placed in a shaker incubator with 100 rpm seed at temperature of 37 °C. After each process of digestion, filter

paper gently wiped off any moisture from the medium surrounding the beads before they were weighed. Eq. (4) helped to establish how much weight had been added or lost by change in mass (Wong et al., 2021).

$$\text{Swelling}\ (\%) = W_S - W_B/W_S \times 100 \quad (4)$$

where W_S was the weight of swollen beads and W_B was the weight of dry beads.

2.8. Fourier transform infrared (FT-IR) spectroscopy

The IR analysis of hydrolysates and loaded beads was performed using an FTIR spectrophotometer. These samples were grinded with KBr, and their spectral scanning was done within the range of 400–4000 cm^{-1} (Stoica et al., 2013).

2.9. Scanning electron microscopy (SEM)

The samples' morphological structure was examined under scanning electron microscopy (SEM) operating at a voltage of 10 kV. The frozen samples were coated with gold (Au), following which they were assessed using an SEM instrument (Li et al., 2021).

2.10. Statistical analysis

Enzymatic hydrolysis was done using Design Expert software version 11 and response surface methodology in the form of central compound design. Data analysis was done with SPSS software version 26, in the form of a completely randomized design using one-way analysis of variance (ANOVA). The comparison of values was checked with Duncan's multiple-range test at a 95% confidence level, and graphs were drawn with Excel 2019 and Origin 2019 software. All tests were performed in three replicates.

3. Results and discussion

3.1. Antioxidant activity of PSPH

According to Fig. 1, the highest amount of antioxidant activity for pancreatin hydrolysate based on DPPH free radical scavenging activity, iron ion chelation activity, and total antioxidant activity (absorbance at 695 nm) was 52.6 ± 2.1%, 91.1 ± 3.9% and 1.0 ± 0.1, and for alcalase was 52% ± 2.1, 93 ± 4.42% and 0.711 ± 0.08, respectively. According to the results, pancreatin hydrolysates showed higher antioxidant activities in DPPH free radical scavenging and total antioxidant activity, so this sample was chosen as the core material for encapsulation. The highest amount of antioxidant activity belonged to the time of 105 min and the ratio of 1.5% E/S. In other words, the amount of antioxidant activity decreased with increasing time. It can be stated that, probably due to the continuation of the hydrolysis process and the effect of the enzyme on the hydrolysates produced in the early stages, it has led to the destruction of the hydrolysates with high antioxidant capacity (MESHGINFAR et al., 2014). Shaban Pour et al. (2017), Kaveh et al. (2019), and Ovissipour et al. (2009) reported that by increasing time, the amount of antioxidant activity decreased. On the other hand, by increasing the concentration of the enzyme up to 1.5%, the amount of antioxidant activity decreased. This is due to excessive protein hydrolysis, which causes the complete release of hydrophilic amino acids and makes it difficult to react active amino acids with the fat-soluble DPPH free radical (Zhu et al., 2008). Also, higher concentrations of E/S may destroy the hydrolysates with electron-donating properties and Fe chelation activity, which reduce the antioxidant activity.

3.2. Encapsulation efficiency

As it can be seen from Fig. 2, the highest amount of encapsulation efficiency (85.06 ± 2.54%) belonged to CMC-alginate, and the lowest one (71.63 ± 2.15%) belonged to plain alginate. According to the results, there were significant differences between EE of the plain alginate (71.63 ± 2.15%), CMC-alginate (85.06 ± 2.54%), Tragacanth-alginate (80.4 ± 2.3%), and Aloe-alginate (75.63 ± 2.1%) ($p < 0.05$). Divalent cations such as calcium ions, by connecting alginate chains, form a network with cross-ionic bonds, which leads to the formation of a gel-alginate solution (George and Abraham, 2007). Calcium alginate hydrogel by itself is very fragile and has poor mechanical properties. There are many hydroxyl groups in CMC that, in addition to high water absorption, can establish hydrogen bonds with alginate molecules to increase the durability of the hydrogel (He et al., 2021). On the other hand, the cross-links between carboxyl groups in Tragacanth increase stability (Qasemi and Ghaemy, 2020; Sahraei and Ghaemy, 2017). It should be noted that the reduction in encapsulation efficiency is due to an increase in the density of cross-links, which causes a rigid structure, and a decrease in volume in the polymer matrix (Nagarjuna et al., 2016). In some studies that have been conducted on different polysaccharides, the combination of them increased the efficiency of encapsulation, which is probably due to the creation of cross-links between polysaccharides and increasing the stability of hydrogels. For example, Maqsoudlou et al. (2020) investigated the stability and structural properties of encapsulated bee pollen protein hydrolysates with maltodextrin and whey protein. Their results showed that the combination of maltodextrin and whey protein leads to the highest amount of encapsulation efficiency, and maltodextrin by itself causes the lowest amount of it. Rao et al. (2016) performed the encapsulation of casein hydrolysates by using a maltodextrin-gum Arabic combination and reported that the combination of these two gums led to the highest micro-encapsulation efficiency.

3.3. Release rate in the simulated gastrointestinal condition

According to Fig. 3A, the release rate in the gastric environment increased with time for all treatments. The highest amount of release was at 120 min (30.23 ± 0.4%), and the lowest amount was at 30 min (5.3 ± 0.11%). The amount of release in Aloe-alginate and Tragacanth-alginate hydrogels was not significantly different in 60 and 90 min ($P > 0.05$). Also, the highest amount of release belonged to plain alginate, and the lowest amount belonged to CMC-alginate. According to Fig. 3B, by increasing time, the amount of release in the intestine environment increased, and the results showed that the highest amount of release was at 240 min (52.26 ± 0.63%), and the lowest amount was at 60 min (13.46 ± 0.18%). It should be noted that, the highest release amount belonged to plain alginate, and the lowest amount belonged to CMC-alginate. The results showed that the addition of other polysaccharides to alginate increases the cross-links and, as a result, increases the stability of the hydrogel, which preserves the bioactive compound inside the hydrogel. These results are similar to the findings of Bogdanova et al. (2022). During a study, they also added some gelatin to increase the stability of calcium alginate hydrogel, which increased cell viability, the ionic bond, and controlled release. Sodium alginate, in the presence of divalent cations, exhibits unique gelling properties in aqueous solutions, but the gel has limitations such as instability and fragility. The combination of sodium alginate with different polymers causes stable and controlled release, high porosity, and multiple responses (Zou et al., 2020). CMC is one of the synthetic polymers that are created by polymerization cross-linking or physicochemical cross-linking, which have advantages such as high mechanical strength and physicochemical stability and is used with alginate to increase the stability of the hydrogel (Wang et al., 2013; Xu et al., 2018). Alginate-CMC hydrogels, based on two polyanionic polysaccharides, are sensitive to pH in the weak alkaline environment of the intestine and prevent the leakage of the bioactive compound and the bursting of the hydrogel in the gastric environment (Hu et al., 2021). In the present study, the release amount in the alginate-tragacanth sample was lower than the release amount in

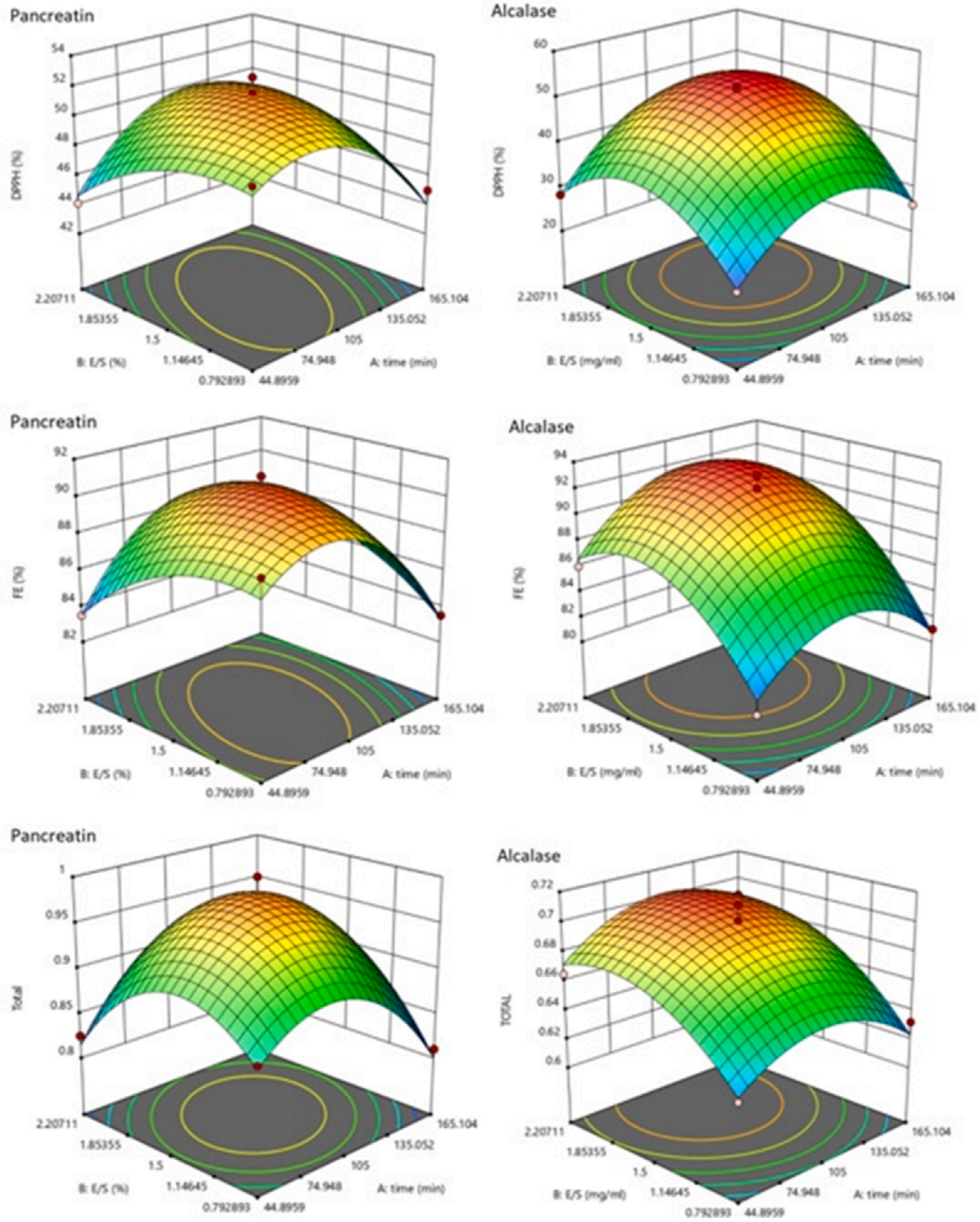

Fig. 1. Antioxidant activity of pumpkin seed protein hydrolysates (PSPH).

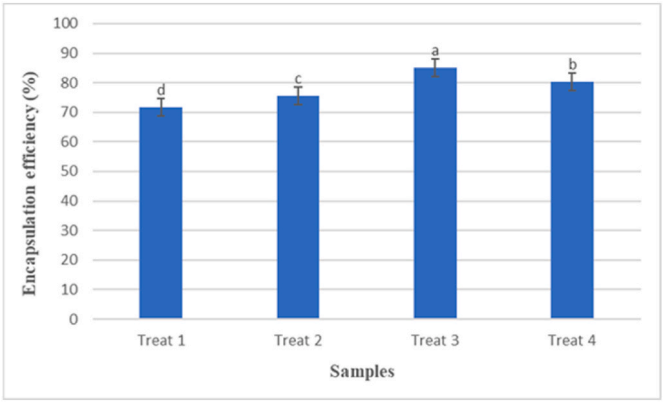

Fig. 2. Encapsulation efficiency of PSPH of different hyrogel. Treat1: Alginate, Treat 2: Aloe-alginate, Treat 3: CMC-alginate, and Treat 4: Tragacanth-alginate. Data represent as mean value ± SD of at least three replicates.

the control sample (alginate), which is different from the results announced by Nagarjuna et al. (2016), who reported that the release amount in the control sample was the lowest amount. In the current study, probably due to the creation of cross-links, the hydrogel wall has become more stable and stronger, and the release amount has decreased compared to the control sample (alginate). Also, Chelu et al. (2023) reported that the presence of aloe Vera in the gel structure gives good consistency and plasticity to the hydrogel. In medical science, due to the pharmacological importance of sodium alginate and aloe Vera, the ionotropic gelation of these polysaccharides constitutes a potential double drug delivery system (Singh et al., 2012).

3.4. Antioxidant activity in the simulated gastrointestinal condition

According to Fig. 4, the total antioxidant capacity of all samples decreased during the digestion period in the simulated gastric and intestine environments. According to Fig. 4A, the highest amount of total antioxidant activity (absorbance at 695 nm) in a simulated gastric environment belonged to free PSPH (0.98 ± 0.12), and the lowest amount belonged to CMC-alginate (0.73 ± 0.08). According to Fig. 4B, the highest amount of total antioxidant activity (absorbance at 695 nm)

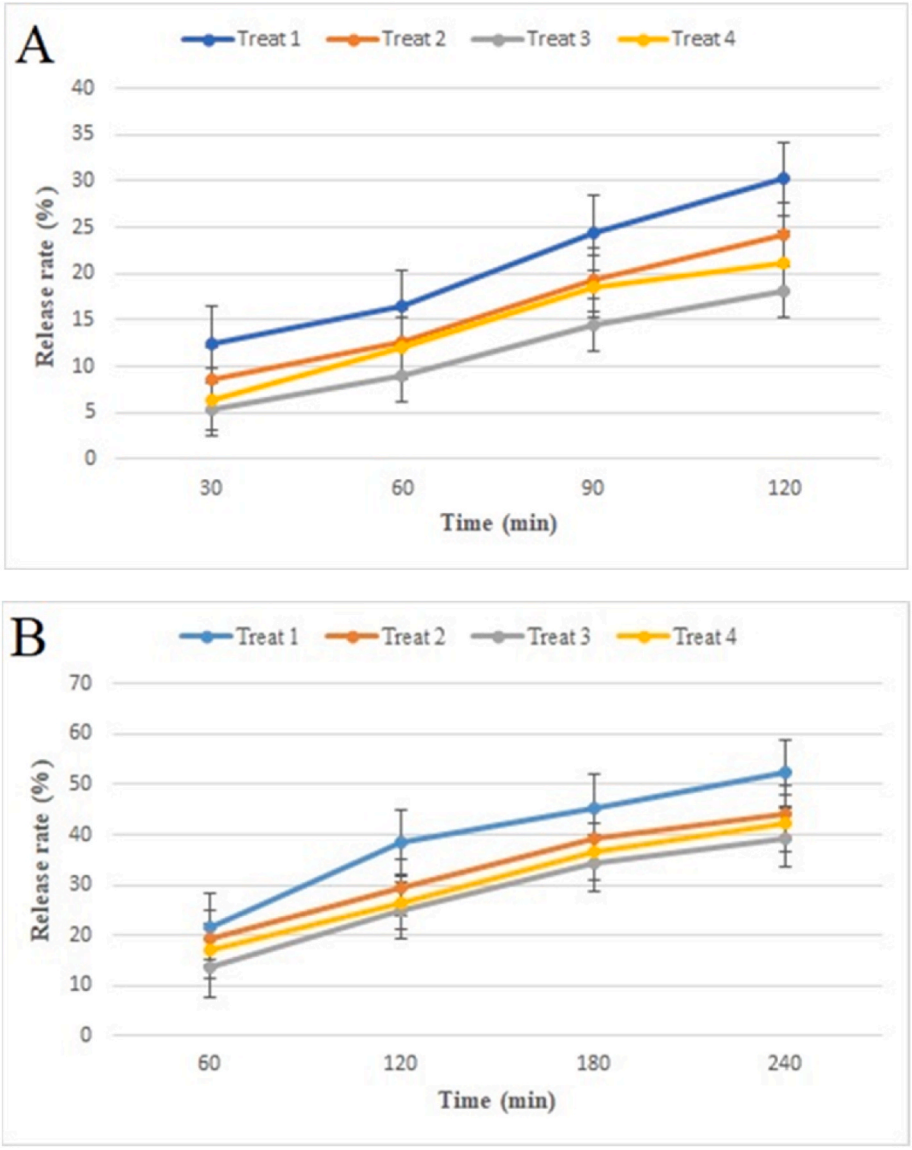

Fig. 3. The release patterns of hydrogel contained PSPH in A, simulated gastric condition, and B, simulated intestinal condition. Treat 1: Alginate; Treat 2: Aloe-alginate; Treat 3: CMC-alginate; and Treat 4: Tragacanth-alginate. Data represent a mean value ± SD of at least n = 3.

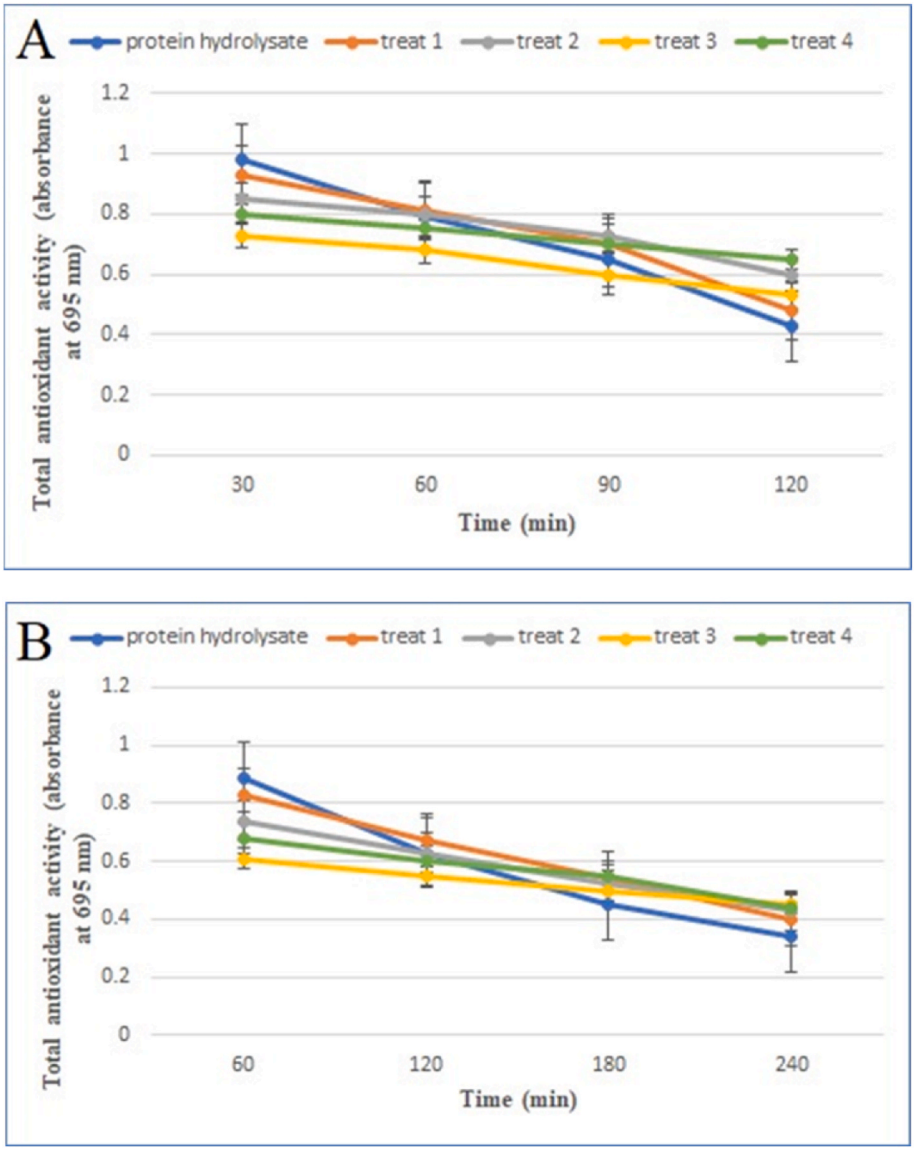

Fig. 4. The total antioxidant patterns of free PSPH and hydrogel contained PSPH in A, simulated gastric condition, and B, simulated intestinal condition. Treat 1: Alginate; Treat 2: Aloe-alginate; Treat 3: CMC-alginate; and Treat 4: Tragacanth-alginate. Data represent a mean value ± SD of at least n = 3.

in the simulated intestinal environment belonged to free PSPH (0.89 ± 0.1), and the lowest amount belonged to CMC-alginate (0.61 ± 0.05). On the other hand, after digestion time, the highest decrease was related to PSPH (0.43 ± 0.04 and 0.34 ± 0.03, respectively, in the gastric and intestinal environments). So that after 2 h of digestion in the gastric environment and after 4 h of digestion in the intestinal environment, its total antioxidant capacity was reduced by 56.1% and 61.8% respectively. On the other hand, the lowest rate of reduction was related to CMC-alginate treatment, so that the total antioxidant capacity after gastric and intestinal digestion decreased by 27.4% and 26.2%, respectively. Among hydrogels, the highest reduction in antioxidant capacity was related to plain alginate, and the lowest amount belonged to CMC-alginate. The results showed that the formulation investigated in this research has a suitable ability to reduce the instability of the PSPH. Similar to these findings, Liang et al. (2016), by microencapsulation of epigallocatechin gallate inside niosomal vesicles and investigating its iron ion reduction property during digestion in simulated intestinal conditions, reported that the amount of antioxidant activity of the free and micro-encapsulated compounds within 2 h of digestion in the intestine decreased, but this decrease was less in the microencapsulated sample. Also, Hu et al. (2017) reported that by microencapsulating orange peel flavonoid compounds in pectin nanoparticles, their antioxidant power decreased during digestion in simulated intestinal conditions, and this decrease was greater in free flavonoid compared to microencapsulated flavonoid.

3.5. Swelling in the simulated gastrointestinal condition

According to Fig. 5A, the highest amount of swelling in the simulated gastric condition belonged to CMC-Alginate (−13.77 ± 0.21%) and the lowest amount belonged to alginate hydrogel (−23.43 ± 0.18%). On the other hand, according to Fig. 5B, the highest amount of swelling in the simulated intestine condition belonged to CMC-alginate (39.57 ± 0.45%) and the lowest amount belonged to alginate hydrogel (25.43 ± 0.3%). It has been reported that the amount of water absorption affects the release rate of trapped molecules and the laboratory degradation of hydrophilic polymers (Göpferich, 1996). Hydrogels can reversibly absorb large amounts of water and other liquids. However, the extent of this property depends on composition as well as cross-linking (Bialik-Wąs et al., 2022). The low swelling amount of alginate hydrogel is probably caused by a matrix with weak transverse connections. More swelling in the intestine environment compared to the gastric

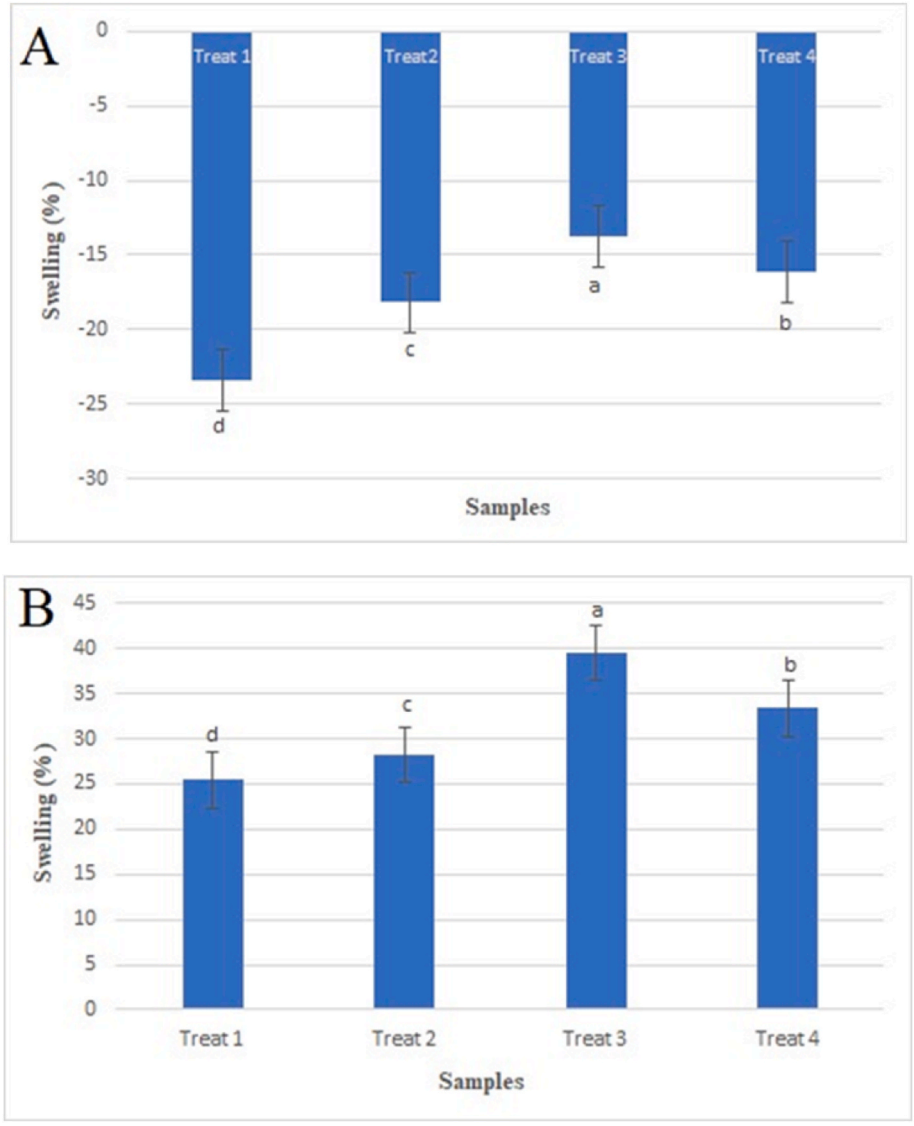

Fig. 5. The swelling amount of hydrogel contained PSPH in A, simulated gastric condition, and B, simulated intestinal condition. Treat 1: Alginate; Treat 2: Aloe-alginate; Treat 3: CMC-alginate; and Treat 4: Tragacanth-alginate. Data represent a mean value ± SD of at least n = 3.

environment is due to the formation of ions with the same charge, which leads to electrostatic repulsion between COO^- groups and an increase in the size of the mesh (Turan and Caykara, 2007). The degree of swelling is due to the increase in hydrophilicity and the change in the ratio of sodium alginate, which determines the cross-linking density and swelling of the resulting polymer (Singh and Singh, 2021). In an acidic environment, carboxyl residues are protonated. Therefore, the repulsive forces decrease and lead to the contraction of the matrix, and reducing its swelling (Ramos et al., 2018). In the intestinal environment, loss of hydrogen balance and changes in ionic strength weaken the microparticle structure. Most microparticles swell slightly due to internal electrostatic repulsive interactions between carboxyl groups with a partial negative charge in polysaccharide chains (Tsirigotis-Maniecka, 2020) (see Fig. 6).

3.6. Fourier transform infrared (FTIR)

According to Fig. 6A, all samples showed stretching vibrations of O–H bonds and asymmetric and symmetric stretching vibrations of the carboxylate group in 3400, 1600, and 1400 (cm^{-1}), respectively. In addition, the spectra showed C–O stretching vibrations in the range of 1000–1100 (cm^{-1}). The 2100 (cm^{-1}) vibration was attributed to the symmetric O–H stretching. The vibrations of 3400 (cm^{-1}) belonged to NH, O–H stretching, and those of 2200 (cm^{-1}) belonged to C═C groups in protein hydrolysates. 1600, 1400, and 1000 (cm^{-1}) vibrations belonged to C═O stretching and NH bending groups in the first type amide, COO^- stretching in the third type amide, and C–O stretching, respectively. The stretching observed at the lower wavelength belonged to the carbohydrate fraction, which represented the COH group. According to Fig. 6B, all beads that were loaded with protein hydrolysates were shown stretching likeFig. 6A. The appearance of multiple bands instead of a typical band for asymmetric O–H stretching indicates different hydrogen bonding environments resulting from interactions with chloride ions as well as water molecules. Based on the results, FTIR spectroscopy of hydrogels before and after loading of protein hydrolysate showed the same absorption peaks and did not differ from each other. In general, the establishment of hydrogen bonds and electrostatic interactions indicates the successful loading of protein hydrolysates into hydrogels. The results of FTIR were similar to the findings of Ahemen (2013), Araujo et al. (2021), Daemi and Barikani (2012), Kanbargi et al. (2017), Kora and Arunachalam (2012), and Pereira et al. (2011).

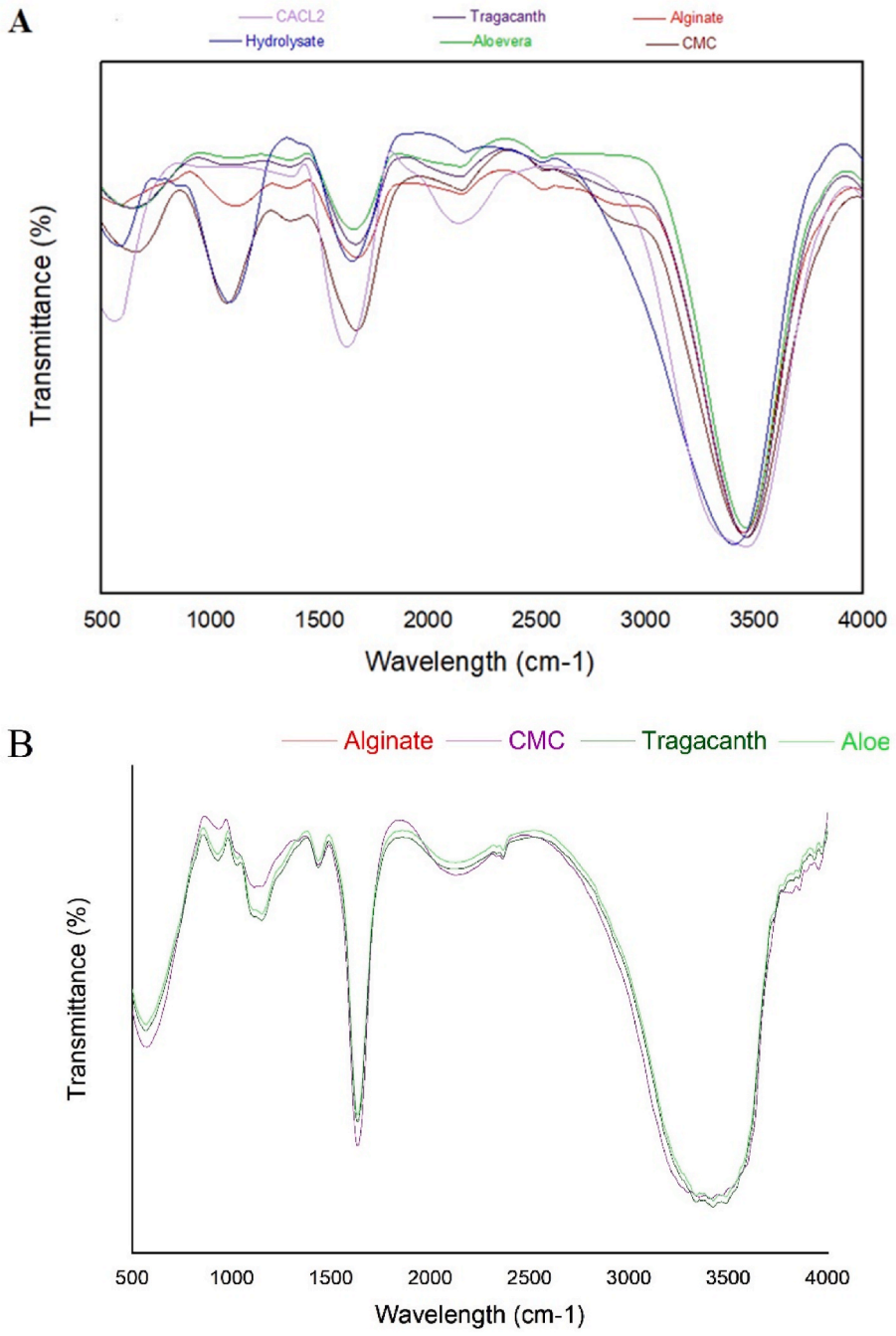

Fig. 6. AFTIR spectra of free Alginate, Tragacanth, $CaCL_2$, CMC, Aloe vera, and PSPH. BFTIR spectra of Alginate loaded with PSPH; CMC-alginate loaded with PSPH; Aloe-alginate loaded with PSPH and Tragacanth-alginate loaded with PSPH.

3.7. Scanning electron microscopy of alginate beads (SEM)

Fig. 7, shows the scanning electron microscopy images of different alginate beads. All treatments were almost spherical. Treatments CMC-alginate, Tragacanth-alginate, and Aloe-alginate had smoother and more polished surfaces than alginate treatment. While the amount of porosity and roughness in plain alginate was higher than in other samples. Analysis of surface morphology showed that the porosity of beads increased with the increase in alginate concentration, their porosity changed according to the hydrogel composition and caused differences in the shape and surface of the produced beads (Lei et al., 2008). The creation of a dense surface may be due to the formation of cross-links between polymers (Nagarjuna et al., 2016). In general, the use of other polymers in combination with alginate reduces the amount of porosity and causes smoother and more uniform surfaces, which is probably due to the unique structure of each polymer and also the interactions between these polymers and alginate.

4. Conclusion

PSPH showed a remarkable antioxidative property and could be used to enhance foods for better health situation. Moreover, it was shown that these hydrolysates can be protected through encapsulation. The encapsulation efficiency of PSPH in plain alginate and beads with Aloe vera, CMC, and tragacanth combinations was 71.63, 75.63, 85.07, and 80.4%, respectively. The release rate of the plain alginate beads was %

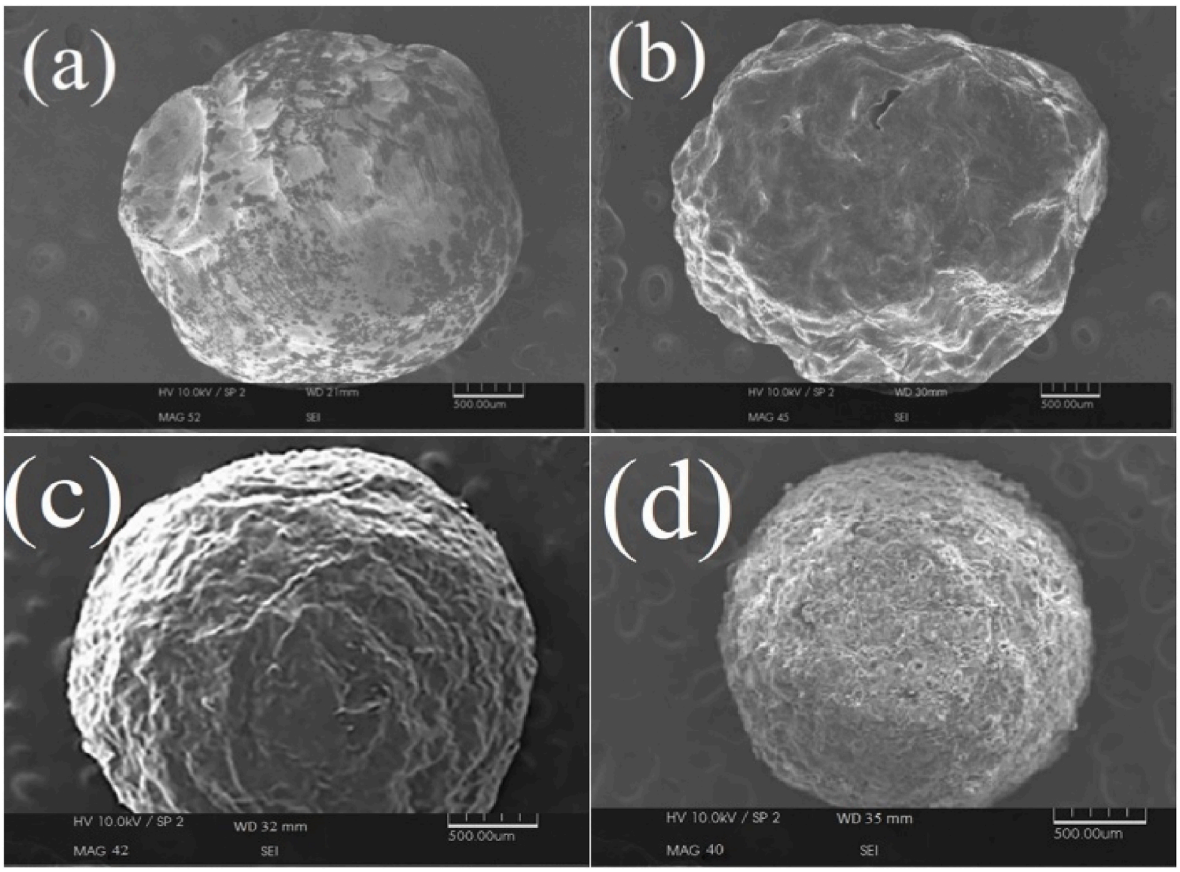

Fig. 7. SEM images of Treat a: Alginate loaded with PSPH; Treat b: CMC-alginate loaded with PSPH; Treat c: Tragacanth-alginate loaded with PSPH; and Treat 4: Aloe-alginate loaded with PSPH.

30.23 in the SGF and %52.26 in the SIF, and decreased in the composite-based beads. The highest decreasing rate in the antioxidant activity during SGI was observed in free PSPH, and the decreasing rate slowed down in the alginate-based composites. The swelling rate in plain alginate was %-23.43 and %25.43 in the SGF and SIF, respectively, and increased in the composite-based beads. The findings revealed that compared to plain alginate, these composite alginate-based hydrogels improved their encapsulation efficiency, protecting bioactive compounds against degradation processes, improving their stability within simulated gastric environment and releasing them into the intestinal medium. Furthermore, they also displayed higher anti-oxidant stability during SGI. FTIR spectroscopy for hydrogels before and after loading protein hydrolysate showed similar absorption spectra which indicated successful incorporation of protein hydrolysates into hydrogel matrices. Analyzing surface morphology exhibited that the use of other polymers as well as reduction in porosity of beads produced smoother surfaces which were more uniform than using alginate alone. Such data enables the scientist to choose polysaccharides more appropriate for SGI-process and this seems to be the key point that in the development of functional food.

Formatting of funding sources

This research did not receive any specific grant from funding agencies in the public, commercial, or not-for-profit sectors.

Copyright assignment

The undersigned authors transfer all copyright ownership of this manuscript to *Current Research in Food Science*, in the event the work is published. The undersigned authors warrant the article is original, does not infringe upon any copyright or other proprietary right of any third party, is not under consideration for publication by any other journal, and has not been published previously. The authors confirm that they have reviewed and approved the final version of the manuscript.

Author agreement

We the undersigned declare that this manuscript is original, has not been published before and is not currently being considered for publication elsewhere.

We confirm that the manuscript has been read and approved by all named authors and that there are no other persons who satisfied the criteria for authorship but are not listed. We further confirm that the order of authors listed in the manuscript has been approved by all of us.

We understand that the Corresponding Author is the sole contact for the Editorial process. He is responsible for communicating with the other authors about progress, submissions of revisions and final approval of proofs.

CRediT authorship contribution statement

Zeinab Nooshi Manjili: Conceptualization, Methodology, Software, Validation, Formal analysis, Investigation, Data curation, Writing – original draft. **Alireza Sadeghi Mahoonak:** Conceptualization, Methodology, Validation, Investigation, Resources, Data curation, Writing – review & editing, Supervision, Project administration, Funding acquisition. **Mohammad Ghorbani:** Methodology, Validation, Writing – review & editing. **Hoda Shahiri Tabarestani:** Methodology, Validation, Writing – review & editing. **Vahid Erfani Moghadam:** Methodology, Validation, Writing – review & editing.

Declaration of competing interest

The authors declare that they have no known competing financial interests or personal relationships that could have appeared to influence the work reported in this paper.

Data availability

Data will be made available on request.

Acknowledgements

The authors wish to thank research section, Gorgan University of Agricultural Sciences and Natural Resources, Gorgan, Iran for their valuable supports.

References

Ahemen, I., 2013. Effect of sodium carboxymethyl cellulose concentration on the photophysical properties of zinc sulfide nanoparticles. Br. J. Appl. Sci. Technol. 3 (4), 1228–1245.
Ahmed, E.M., 2015. Hydrogel: preparation, characterization, and applications: a review. J. Adv. Res. 6 (2), 105–121.
Aktaş, N., Uzlaşır, T., Tunçil, Y.E., 2018. Pre-roasting treatments significantly impact thermal and kinetic characteristics of pumpkin seed oil. Thermochim. Acta 669, 109–115.
Ali, S., Anjum, M.A., Khan, A.S., Nawaz, A., Ejaz, S., Khaliq, G., Iqbal, S., Ullah, S., Rehman, R.N.U., Ali, M.M., 2022. Carboxymethyl cellulose coating delays ripening of harvested mango fruits by regulating softening enzymes activities. Food Chem. 380, 131804.
Alvarado, Y., Muro, C., Illescas, J., Díaz, M.d.C., Riera, F., 2019. Encapsulation of antihypertensive peptides from whey proteins and their releasing in gastrointestinal conditions. Biomolecules 9 (5), 164.
Amin, M.Z., Islam, T., Uddin, M.R., Uddin, M.J., Rahman, M.M., Satter, M.A., 2019. Comparative study on nutrient contents in the different parts of indigenous and hybrid varieties of pumpkin (Cucurbita maxima Linn.). Heliyon 5 (9), 888.
Araujo, J.A., Cortese, Y.J., Mojicevic, M., Brennan Fournet, M., Chen, Y., 2021. Composite films of thermoplastic starch and CaCl2 extracted from eggshells for extending food shelf-life. Polysaccharides 2 (3), 677–690.
Azad, A.K., Al-Mahmood, S.M.A., Chatterjee, B., Wan Sulaiman, W.M.A., Elsayed, T.M., Doolaanea, A.A., 2020. Encapsulation of black seed oil in alginate beads as a ph-sensitive carrier for intestine-targeted drug delivery: in vitro, in vivo and ex vivo study. Pharmaceutics 12 (3), 219.
Aziz, A.R.A., AbouLaila, M.R., Aziz, M., Omar, M.A., Sultan, K., 2018. In vitro and in vivo anthelmintic activity of pumpkin seeds and pomegranate peels extracts against Ascaridia galli. Beni-Suef University Journal of Basic and Applied Sciences 7 (2), 231–234.
Basiri, L., Rajabzadeh, G., Bostan, A., 2017. α-Tocopherol-loaded niosome prepared by heating method and its release behavior. Food Chem. 221, 620–628.
Betancur-Ancona, D., Sandoval-Peraza, M., Arias-Trinidad, A., Gallegos-Tintore, S., Castaneda-Perez, E., Chel-Guerrero, L., 2021. Utilization of Guazuma ulmifolia gum and sodium alginate to form protective beads of antioxidant peptides obtained from Phaseolus lunatus. Food Sci. Technol. 42.
Bialik-Wąs, K., Raftopoulos, K.N., Pielichowski, K., 2022. Alginate hydrogels with aloe vera: the effects of reaction temperature on morphology and thermal properties. Materials 15 (3), 748.
Bogdanova, L., Zelenikhin, P., Makarova, A., Zueva, O., Salnikov, V., Zuev, Y., Ilinskaya, O., 2022. Alginate-based hydrogel as delivery system for therapeutic bacterial RNase. Polymers 14, 2461 s Note: MDPI stays neu-tral with regard to jurisdictional claims in.
Bradford, M.M., 1976. A rapid and sensitive method for the quantitation of microgram quantities of protein utilizing the principle of protein-dye binding. Anal. Biochem. 72 (1–2), 248–254.
Bučko, S., Katona, J., Popović, L., Vaštag, Ž., Petrović, L., Vučinić–Vasić, M., 2015. Investigation on solubility, interfacial and emulsifying properties of pumpkin (Cucurbita pepo) seed protein isolate. LWT–Food Sci. Technol. 64 (2), 609–615.
Bušić, A., Belščak-Cvitanović, A., Cebin, A.V., Karlović, S., Kovač, V., Špoljarić, I., Mršić, G., Komes, D., 2018. Structuring new alginate network aimed for delivery of dandelion (Taraxacum officinale L.) polyphenols using ionic gelation and new filler materials. Food Res. Int. 111, 244–255.
Cano-Sampedro, E., Pérez-Pérez, V., Osorio-Díaz, P., Camacho-Díaz, B., Tapia-Maruri, D., Mora-Escobedo, R., Alamilla-Beltrán, L., 2021. Germinated soybean protein hydrolysate: ionic gelation encapsulation and release under colonic conditions. Rev. Mex. Ing. Quim. 20 (2).
Carpentier, J., Conforto, E., Chaigneau, C., Vendeville, J.-E., Maugard, T., 2022. Microencapsulation and controlled release of α-tocopherol by complex coacervation between pea protein and tragacanth gum: a comparative study with Arabic and tara gums. Innovat. Food Sci. Emerg. Technol. 77, 102951.
Chelu, M., Popa, M., Ozon, E.A., Pandele Cusu, J., Anastasescu, M., Surdu, V.A., Calderon Moreno, J., Musuc, A.M., 2023. High-content aloe vera based hydrogels: physicochemical and pharmaceutical properties. Polymers 15 (5), 1312.
Cho, Y.H., Lee, S.Y., Jeong, D.W., Choi, E.J., Kim, Y.J., Lee, J.G., Yi, Y.H., Cha, H.S., 2014. Effect of pumpkin seed oil on hair growth in men with androgenetic alopecia: a randomized, double-blind, placebo-controlled trial. Evid. base Compl. Alternative Med. 2014.
Daemi, H., Barikani, M., 2012. Synthesis and characterization of calcium alginate nanoparticles, sodium homopolymannuronate salt and its calcium nanoparticles. Sci. Iran. 19 (6), 2023–2028.
Desai, K., Wei, H., Lamartiniere, C., 1996. The preventive and therapeutic potential of the squalene-containing compound, Roidex, on tumor promotion and regression. Cancer Lett. 101 (1), 93–96.
Fujita, K., Teradaira, R., Nagatsu, T., 1976. Bradykininase Activity of Aloe Extract.
George, M., Abraham, T., 2007. pH sensitive alginate–guar gum hydrogel for the controlled delivery of protein drugs. Int. J. Pharm. 335 (1–2), 123–129.
Gohi, B.F.C.A., Du, J., Zeng, H.-Y., Cao, X.-j., Zou, K.M., 2019. Microwave pretreatment and enzymolysis optimization of the Lotus seed protein. Bioengineering 6 (2), 28.
Gómez-Mascaraque, L.G., Miralles, B., Recio, I., López-Rubio, A., 2016. Microencapsulation of a whey protein hydrolysate within micro-hydrogels: impact on gastrointestinal stability and potential for functional yoghurt development. J. Funct.Foods 26, 290–300.
Göpferich, A., 1996. Mechanisms of polymer degradation and erosion. The Biomaterials: Silver Jubilee Compendium, pp. 117–128.
Guhagarkar, S.A., Malshe, V.C., Devarajan, P.V., 2009. Nanoparticles of polyethylene sebacate: a new biodegradable polymer. AAPS PharmSciTech 10, 935–942.
Hacker, M.C., Mikos, A.G., 2011. Chapter 33 - synthetic polymers. In: Atala, A., Lanza, R., Thomson, J.A., Nerem, R. (Eds.), Principles of Regenerative Medicine, second ed. Academic Press, pp. 587–622. https://doi.org/10.1016/B978-0-12-381422-7.10033-1.
He, X., Zeng, L., Cheng, X., Yang, C., Chen, J., Chen, H., Ni, H., Bai, Y., Yu, W., Zhao, K., 2021. Shape memory composite hydrogel based on sodium alginate dual crosslinked network with carboxymethyl cellulose. Eur. Polym. J. 156, 110592.
Hemmati, K., Masoumi, A., Ghaemy, M., 2016. Tragacanth gum-based nanogel as a superparamagnetic molecularly imprinted polymer for quercetin recognition and controlled release. Carbohydr. Polym. 136, 630–640.
Hirata, T., Suga, T., 1977. Biologically active constituents of leaves and roots of Aloe arborescens var. natalensis. Z. Naturforsch. C Biosci. 32 (9–10), 731–734.
Hosseini, M.S., Hemmati, K., Ghaemy, M., 2016. Synthesis of nanohydrogels based on tragacanth gum biopolymer and investigation of swelling and drug delivery. Int. J. Biol. Macromol. 82, 806–815.
Hu, Y., Hu, S., Zhang, S., Dong, S., Hu, J., Kang, L., Yang, X., 2021. A double-layer hydrogel based on alginate-carboxymethyl cellulose and synthetic polymer as sustained drug delivery system. Sci. Rep. 11 (1), 9142.
Hu, Y., Zhang, W., Ke, Z., Li, Y., Zhou, Z., 2017. In vitro release and antioxidant activity of Satsuma Mandarin (Citrus reticulata Blanco cv. unshiu) peel flavonoids encapsulated by pectin nanoparticles. Int. J. Food Sci. Technol. 52 (11), 2362–2373.
Huang, Y., Zhang, L., Hu, J., Liu, H., 2023. Improved loading capacity and viability of probiotics encapsulated in alginate hydrogel beads by in situ cultivation method. Foods 12 (11), 2256.
Kabiri, K., Omidian, H., Zohuriaan-Mehr, M., Doroudiani, S., 2011. Superabsorbent hydrogel composites and nanocomposites: a review. Polym. Compos. 32 (2), 277–289.
Kanbargi, K.D., Sonawane, S.K., Arya, S.S., 2017. Encapsulation characteristics of protein hydrolysate extracted from Ziziphus jujube seed. Int. J. Food Prop. 20 (12), 3215–3224.
Kaveh, S., Sadeghi, M.A., Ghorbani, M., Jafari, M., Sarabandi, K., 2019. Optimization of factors affecting the antioxidant activity of fenugreek seed's protein hydrolysate by response surface methodology. Iranian Journal of Nutrition Sciences & Food Technology 14 (1).
Kora, A.J., Arunachalam, J., 2012. Green fabrication of silver nanoparticles by gum tragacanth (Astragalus gummifer): a dual functional reductant and stabilizer. J. Nanomater. 2012, 1–8.
Kurt, A., Cengiz, A., Kahyaoglu, T., 2016. The effect of gum tragacanth on the rheological properties of salep based ice cream mix. Carbohydr. Polym. 143, 116–123.
Lei, J., Kim, J.-H., Jeon, Y.S., 2008. Preparation and properties of alginate/polyaspartate composite hydrogels. Macromol. Res. 16, 45–50.
Li, Q., Duan, M., Hou, D., Chen, X., Shi, J., Zhou, W., 2021. Fabrication and characterization of Ca (II)-alginate-based beads combined with different polysaccharides as vehicles for delivery, release and storage of tea polyphenols. Food Hydrocolloids 112, 106274.
Liang, R., Chen, L., Yokoyama, W., Williams, P.A., Zhong, F., 2016. Niosomes consisting of tween-60 and cholesterol improve the chemical stability and antioxidant activity of (−)-epigallocatechin gallate under intestinal tract conditions. J. Agric. Food Chem. 64 (48), 9180–9188.
Lorenzetti, L.J., Salisbury, R., Beal, J.L., Baldwin, J.N., 1964. Bacteriostatic property of Aloe vera. J. Pharmaceut. Sci. 53, 1287.
Lu, D., Peng, M., Yu, M., Jiang, B., Wu, H., Chen, J., 2021. Effect of enzymatic hydrolysis on the zinc binding capacity and in vitro gastrointestinal stability of peptides derived from pumpkin (Cucurbita pepo L.) seeds. Front. Nutr. 8, 647782.
Maqsoudlou, A., Mahoonak, A.S., Mohebodini, H., Koushki, V., 2020. Stability and structural properties of bee pollen protein hydrolysate microencapsulated using maltodextrin and whey protein concentrate. Heliyon 6 (5), 888.
Mazloomi-Kiyapey, S.N., Sadeghi-Mahoonak, A., Ranjbar-Nedamani, E., Nourmohammadi, E., 2019. Production of antioxidant peptides through hydrolysis of medicinal pumpkin seed protein using pepsin enzyme and the evaluation of their functional and nutritional properties. Arya Atherosclerosis 15 (5), 218.
Medina-Torres, L., Núñez-Ramírez, D., Calderas, F., González-Laredo, R., Minjares-Fuentes, R., Valadez-García, M., Bernad-Bernad, M., Manero, O., 2019.

Microencapsulation of gallic acid by spray drying with aloe vera mucilage (aloe barbadensis miller) as wall material. Ind. Crop. Prod. 138, 111461.
Meshginfar, N., Sadeghi, M.A., Ziaiifar, A., Ghorbani, M., Kashaninejad, M., 2014. Optimization Of The Production of Protein Hydrolysates From Meat Industry by Products by Response Surface Methodology.
Nagarjuna, G., Kumara Babu, P., Maruthi, Y., Parandhama, A., Madhavi, C., Subha, M., 2016. Sodium alginate/tragacanth gum blend hydrogel membranes for controlled release of verapamil hydrochloric acid. Indian J. Adv. Chem. Sci. 4, 469–477.
Nourmohammadi, E., Sadeghi Mahoonak, A., Ghorbani, M., Alami, M., Sadeghi, M., 2017. The optimization of the production of anti-oxidative peptides from enzymatic hydrolysis of Pumpkin seed protein. Iranian Food Science and Technology Research Journal 13 (1), 14–26.
Ovissipour, M., Abedian, A., Motamedzadegan, A., Rasco, B., Safari, R., Shahiri, H., 2009. The effect of enzymatic hydrolysis time and temperature on the properties of protein hydrolysates from Persian sturgeon (Acipenser persicus) viscera. Food Chem. 115 (1), 238–242.
Pereira, R., Tojeira, A., Vaz, D.C., Mendes, A., Bártolo, P., 2011. Preparation and characterization of films based on alginate and aloe vera. Int. J. Polym. Anal. Char. 16 (7), 449–464.
Perez, R.A., Kim, M., Kim, T.-H., Kim, J.-H., Lee, J.H., Park, J.-H., Knowles, J.C., Kim, H.-W., 2014. Utilizing core–shell fibrous collagen-alginate hydrogel cell delivery system for bone tissue engineering. Tissue Eng. 20 (1–2), 103–114.
Prasathkumar, M., Sadhasivam, S., 2021. Chitosan/Hyaluronic acid/Alginate and an assorted polymers loaded with honey, plant, and marine compounds for progressive wound healing—know-how. Int. J. Biol. Macromol. 186, 656–685.
Prieto, P., Pineda, M., Aguilar, M., 1999. Spectrophotometric quantitation of antioxidant capacity through the formation of a phosphomolybdenum complex: specific application to the determination of vitamin E. Anal. Biochem. 269 (2), 337–341.
Qasemi, S., Ghaemy, M., 2020. Novel superabsorbent biosensor nanohydrogel based on gum tragacanth polysaccharide for optical detection of glucose. Int. J. Biol. Macromol. 151, 901–908.
Ramos, P.E., Silva, P., Alario, M.M., Pastrana, L.M., Teixeira, J.A., Cerqueira, M.A., Vicente, A.A., 2018. Effect of alginate molecular weight and M/G ratio in beads properties foreseeing the protection of probiotics. Food Hydrocolloids 77, 8–16.
Rao, P.S., Bajaj, R.K., Mann, B., Arora, S., Tomar, S., 2016. Encapsulation of antioxidant peptide enriched casein hydrolysate using maltodextrin–gum Arabic blend. J. Food Sci. Technol. 53, 3834–3843.
Rezig, L., Riaublanc, A., Chouaibi, M., Guéguen, J., Hamdi, S., 2016. Functional properties of protein fractions obtained from pumpkin (Cucurbita maxima) seed. Int. J. Food Prop. 19 (1), 172–186.
Robson, M.C., Heggers, J.P., Hagstrom, W.J., 1982. Myth, magic, witchcraft, or fact? Aloe vera revisited. J. Burn Care Rehabil. 3 (3), 157–163.
Sahraei, R., Ghaemy, M., 2017. Synthesis of modified gum tragacanth/graphene oxide composite hydrogel for heavy metal ions removal and preparation of silver nanocomposite for antibacterial activity. Carbohydr. Polym. 157, 823–833.
Seyger, M., Van De Kerkhof, P., van Vlijmen-Willems, I., De Bakker, E., Zwiers, F., De Jong, E., 1998. The efficacy of a new topical treatment for psoriasis: mirak. J. Eur. Acad. Dermatol. Venereol. 11 (1), 13–18.
Shaban Pour, B., Kord Jazi, M., Nazari, K., Esmaeeli Khariki, M., 2017. Effect of enzymatic hydrolysis time, temperature and enzyme to substrate ratio on antioxidant properties of prawn bioactive peptides. J. Food Sci. Technol. 14 (62), 45-31.
Shah, P., 2020. Polymers in food. In: Polymer Science and Innovative Applications. Elsevier, pp. 567–592.
Simas-Tosin, F., Wagner, R., Santos, E., Sassaki, G., Gorin, P., Iacomini, M., 2009. Polysaccharide of nectarine gum exudate: comparison with that of peach gum. Carbohydr. Polym. 76 (3), 485–487.
Singh, B., Sharma, V., Dhiman, A., Devi, M., 2012. Design of Aloe vera-alginate gastroretentive drug delivery system to improve the pharmacotherapy. Polym.-Plast. Technol. Eng. 51 (13), 1303–1314.
Singh, B., Singh, J., 2021. Application of tragacanth gum and alginate in hydrogel wound dressing's formation using gamma radiation. Carbohydrate Polymer Technologies and Applications 2, 100058.
Sitohy, M.Z., Desoky, E.-S.M., Osman, A., Rady, M.M., 2020. Pumpkin seed protein hydrolysate treatment alleviates salt stress effects on Phaseolus vulgaris by elevating antioxidant capacity and recovering ion homeostasis. Sci. Hortic. 271, 109495.
Stoica, R., Pop, S., Ion, R., 2013. Evaluation of natural polyphenols entrapped in calcium alginate beads prepared by the ionotropic gelation method. J. Optoelectron. Adv. Mater. 15 (7–8), 893–898.
Su, Y.-T., Chang, H.-L., Shyue, S.-K., Hsu, S.-L., 2005. Emodin induces apoptosis in human lung adenocarcinoma cells through a reactive oxygen species-dependent mitochondrial signaling pathway. Biochem. Pharmacol. 70 (2), 229–241.
Sun, X.-Z., Wang, X., Wu, J.-Z., 2017. Development of thermosensitive microgel-loaded cotton fabric for controlled drug release. Appl. Surf. Sci. 403, 509–518.
Swamy, B.Y., Yun, Y.-S., 2015. In vitro release of metformin from iron (III) cross-linked alginate–carboxymethyl cellulose hydrogel beads. Int. J. Biol. Macromol. 77, 114–119.
Tsirigotis-Maniecka, M., 2020. Alginate-, carboxymethyl cellulose-, and κ-carrageenan-based microparticles as storage vehicles for cranberry extract. Molecules 25 (17), 3998.
Turan, E., Caykara, T., 2007. Swelling and network parameters of pH-sensitive poly (acrylamide-co-acrylic acid) hydrogels. J. Appl. Polym. Sci. 106 (3), 2000–2007.
Wang, B.-l., Ren, K.-f., Chang, H., Wang, J.-l., Ji, J., 2013. Construction of degradable multilayer films for enhanced antibacterial properties. ACS Appl. Mater. Interfaces 5 (10), 4136–4143.
Wong, S.K., Lawrencia, D., Supramaniam, J., Goh, B.H., Manickam, S., Wong, T.W., Pang, C.H., Tang, S.Y., 2021. In vitro digestion and swelling kinetics of thymoquinone-loaded pickering emulsions incorporated in alginate-chitosan hydrogel beads. Front. Nutr. 8, 752207.
Xu, J., Liu, X., Ren, X., Gao, G., 2018. The role of chemical and physical crosslinking in different deformation stages of hybrid hydrogels. Eur. Polym. J. 100, 86–95.
Yagi, A., Kabash, A., Mizuno, K., Moustafa, S., Khalifa, T., Tsuji, H., 2003. Radical scavenging glycoprotein inhibiting cyclooxygenase-2 and thromboxane A2 synthase from Aloe vera gel. Planta Med. 69 (3), 269–271.
Yu, K., Zhou, L., Xu, J., Jiang, F., Zhong, Z., Zou, L., Liu, W., 2022. Carboxymethyl cellulose-based water barrier coating regulated postharvest quality and ROS metabolism of pakchoi (Brassica chinensis L.). Postharvest Biol. Technol. 185, 111804.
Zhang, M., Zhao, X., 2020. Alginate hydrogel dressings for advanced wound management. Int. J. Biol. Macromol. 162, 1414–1428.
Zhu, L., Chen, J., Tang, X., Xiong, Y.L., 2008. Reducing, radical scavenging, and chelation properties of in vitro digests of alcalase-treated zein hydrolysate. J. Agric. Food Chem. 56 (8), 2714–2721.
Zou, Z., Zhang, B., Nie, X., Cheng, Y., Hu, Z., Liao, M., Li, S., 2020. A sodium alginate-based sustained-release IPN hydrogel and its applications. RSC Adv. 10 (65), 39722–39730.